Chem Soc Rev

TUTORIAL REVIEW

Photoelectrochemical hydrogen production from biomass derivatives and water

Cite this: DOI: 10.1039/c3cs60392j

Xihong Lu, Shilei Xie, Hao Yang, Yexiang Tong and Hongbing Ji*

Hydrogen, a clean energy carrier with high energy capacity, is a very promising candidate as a primary energy source for the future. Photoelectrochemical (PEC) hydrogen production from renewable biomass derivatives and water is one of the most promising approaches to producing green chemical fuel. Compared to water splitting, hydrogen production from renewable biomass derivatives and water through a PEC process is more efficient from the viewpoint of thermodynamics. Additionally, the carbon dioxide formed can be re-transformed into carbohydrates *via* photosynthesis in plants. In this review, we focus on the development of photoanodes and systems for PEC hydrogen production from water and renewable biomass derivatives, such as methanol, ethanol, glycerol and sugars. We also discuss the future challenges and opportunities for the design of the state-of-the-art photoanodes and PEC systems for hydrogen production from biomass derivatives and water.

Received 1st November 2013

DOI: 10.1039/c3cs60392j

www.rsc.org/csr

Key learning points

(1) Basic principles of PEC hydrogen from biomass derivatives and water.
(2) The common photoanodes used in PEC hydrogen from biomass derivatives.
(3) Typical biomass derivatives for PEC hydrogen production.
(4) The opportunities and challenges of PEC hydrogen from biomass derivatives and water.

1. Introduction

With the fast development of the global economy and population, the energy crisis has become one of the great challenges in the 21st century. Today, most of the energy supplies (more than 80%) are based on fossil fuels, such as coal, oil, natural gas, *etc.* The excessive depletion of fossil fuels has raised severe environmental pollution. On the other hand, fossil fuels are non-renewable resources since they take millions of years to form, and reserves are being depleted much faster than new ones are being made.[1] Hydrogen is considered as an ideal energy carrier for the future because it is efficient and clean burning with water vapor as the only by-product. The specific energy density of hydrogen is much higher than any other conventional fuel such as gasoline. For example, one gram of hydrogen could release about 140 kJ of energy, which is about four times higher than that of methane (33 kJ g^{-1}).[2]

The essential factor to the success of realizing a hydrogen economy is the sustainable supply of hydrogen. Today, there are two primary methods to produce hydrogen for commercial use. One is hydrocarbon reformation, which employs heat to separate hydrogen from a carrier, usually a fossil fuel such as natural gas. Most of the current hydrogen produced comes from steam methane reforming (SMR). For example, about 95% of commercial hydrogen produced in the U.S. is made *via* SMR.[1] Heat is necessary during this process and the generation of heat typically involves combustion of a fossil fuel. Therefore, hydrogen production through this approach is not only energy intensive, but also emits undesired CO_2. The second approach is electrolysis, which separates the hydrogen from a hydrogen carrier through electricity. The energy efficiency of electrolysis reaches levels higher than 70%, but it suffers from high cost. It is estimated that the production cost is about \$20.0 per GJ of hydrogen. Therefore, developing the techniques of sustainable and economic production of hydrogen from renewable resources, such as biomass and water, has become increasingly important.

Photocatalytic (PC)/photoelectrochemical (PEC) water splitting are emerging as the promising and environmental methods for solar hydrogen generation, and have attracted increasing interest. This is because water splitting is a clean reaction without any CO_2 emission and solar energy is a very clean, high-power and

Department of Chemical Engineering, MOE of the Key Laboratory of Bioinorganic and Synthetic Chemistry, School of Chemistry and Chemical Engineering, The Key Lab of Low-carbon Chemistry & Energy Conservation of Guangdong Province, Sun Yat-Sen University, Guangzhou 510275, People's Republic of China

renewable source. Since Fujishima and Honda reported the photoelectrocatalytic hydrogen production from water over TiO_2 semiconductor electrode in 1972,[2] considerable effort has been paid to the development of highly efficient photocatalysts and photoelectrodes. Exciting progress has been made in both the design and fabrication of the photocatalysts and photoelectrodes for water splitting, which are summarized in a review.[3] Despite extensive research effort, the current efficiency of producing hydrogen directly from water is still very low. The addition of sacrificial reagents, such as methanol, Na_2S, Na_2SO_3 and EDTA, can enhance the efficiency to some extent, but the improvement is at the cost of non-renewable sacrificial reagents. Accordingly, PC/PEC production of hydrogen from water presently is quite far from practical application.

Biomass and its derivatives such as methanol, ethanol, glycerol, sugars and methane from biological substrates are potential hydrogen resources since they contain a lot of hydrogen. Moreover, they are regarded as the renewable resources, which can be recycled *via* photosynthesis or photoelectrochemical cells,[4] and the total energy cycle or carbon cycle was summarized in Fig. 1.[5] As a result, biomass and its derivatives have been used for the sustainable production of hydrogen, and recognized as a useful intermediate step to produce hydrogen between the current fossil fuel method and the dream of efficient water splitting. To convert biomass and its derivatives into hydrogen, a lot of processes including steam gasification, fast pyrolysis and supercritical conversion have been developed. However, these processes require rigorous conditions, such as high temperature or high pressure, therefore, leading to high cost.[5] In comparison with these thermochemical processes, PC/PEC reforming of water and biomass derivatives is a more promising approach to generate hydrogen since they can be driven by sunlight and perform under ambient conditions. On the other hand, the calculated changes of Gibbs free energy for hydrogen production from water and biomass derivatives such as methane, ethane, methanol, ethanol formaldehyde, glycerol and glucose are obviously smaller than that for the water splitting. Hence, PC/PEC hydrogen production from these renewable biomass derivatives and water is more efficient than those by PC/PEC water splitting from the viewpoint of thermodynamics.[6]

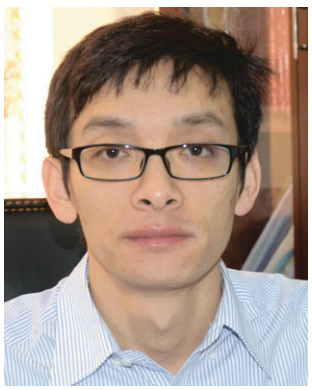

Xihong Lu

Dr Xihong Lu received his BS in Applied Chemistry from Sun Yat-Sen University in 2008, and PhD in Physical Chemistry from Sun Yat-Sen University in 2013. He joined Sun Yat-Sen University as a lecturer of Chemistry in 2013. His current research focuses on the design and synthesis of functional metal oxides and nitrides, and investigation of their fundamental properties and potential applications in energy conversion and storage such as photoelectrochemical water splitting, photocatalytic hydrogen evolution and supercapacitors.

Shilei Xie

Shilei Xie obtained his BS degree in Chemistry of Materials from Sun Yat-Sen University in 2011. He is a graduate student with the Prof. Yexiang Tong at the Sun Yat-Sen University and will get his doctorate in 2015. His research interests are focused on the development and design of nanomaterials and explore their potential applications for photoelectrochemical cell and photocatalysts.

Hao Yang

Hao Yang majored in material chemistry at the school of Chemistry and Chemical Engineering and received his BS degree in 2009 at Sun Yat-Sen University. He joined Professor Ye-Xiang Tong's group in 2012 and became a graduate in the same group. His current research interests focus on the design nanomaterials for fuel cell and solar energy conversion.

Yexiang Tong

Prof. Ye-Xiang Tong received his BS in General Chemistry in 1985, MS in Physical Chemistry in 1988, and PhD in Organic Chemistry in 1999 from Sun Yat-Sen University. He joined Sun Yat-Sen University as an Assistant Professor of Chemistry in 1988. His current research focuses on the electrochemical synthesis of alloys, intermetallic compounds and metal oxide nanomaterials, and investigation of their applications for energy conversion and storage.

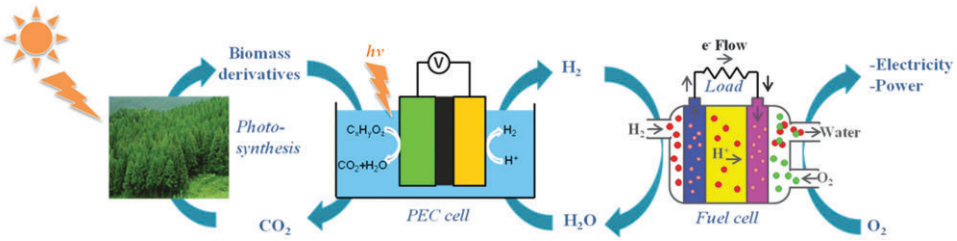

Fig. 1 Carbon neutral cycle with PEC cell and fuel cell.

The use of biomass derivatives and water for solar hydrogen production was first reported by Kawai *et al.* in 1980.[7] They reported that hydrogen could be generated from sugar, starch and cellulose on a $RuO_2/TiO_2/Pt$ photocatalyst under 500 W Xe lamp irradiation. Subsequently, a large number of biomass derivatives such as alcohols, dead insects, and waste materials can also be used to produce hydrogen under the same PC process.[8] Inspired by this work, PC/PEC hydrogen production from biomass derivatives and water has become an active research field over the past few decades. Various attempts have been devoted to enhance the efficiency of these PC/PEC systems. Recent progress in PC hydrogen production from biomass derivatives and water systems have been reviewed well. However, to the best of our knowledge, there are very few reviews in the development of PEC hydrogen production from biomass derivatives and water systems. In this paper, we review the recent progress on the development of PEC hydrogen production from biomass derivatives and also discuss the future challenges and opportunities for the design of the state-of-the-art PEC systems for hydrogen production from biomass derivatives and water.

2. Mechanism for PEC hydrogen from biomass derivatives and water

A PEC cell is made up of a photoactive semiconductor electrode, a counter electrode (*e.g.* Pt or semiconductor), electrolyte and a membrane. In most case, the photoactive electrode is an n-type semiconductor, and the counter electrode is Pt. This n-type semiconductor electrode is usually named "photoanode", on which oxidation reactions take place. The performance of a PEC cell is largely determined by the properties of the photoanode. For example, a photoanode with suitable band edge positions that straddle the redox potential of water can achieve the overall PEC water splitting while others do not. Additionally, the efficiency of water splitting may be significantly enhanced if the photoanode has a small band gap for visible light absorption and fast charge transport. On the other hand, the Schottky barrier formed between the Pt and photoanode can serve as an efficient electron trap to prevent photogenerated electron–hole recombination, and hence promote the photocatalytic reaction. Pt is also an electrocatalyst for H_2 production, in which the trapped photogenerated electrons (e^-) are transferred to protons (H^+) to produce H_2. Additionally, to reduce or avoid the effect of the products that are generated on the anode and cathode surface by the desired reactions, a membrane such as Nafion, glass frit and diaphragm is used as the electrolyte separator between anode and cathode.

Fig. 2a illustrates the mechanism of PEC hydrogen production from biomass-derived oxygenates (denoted as $C_xH_yO_z$) and water over a TiO_2 photoanode. Under irradiation with the photon energy over the band-gap energy of the photoanode, the electrons (e^-) will be excited and promoted from valence band (VB) to conduction band (CB), and then transfer to the Pt cathode through an external circuit, and finally react with H^+ to generate hydrogen. Photoexcited h^+ produced in the VB of the semiconductor will oxidize the $C_xH_yO_z$ to CO_2 and H_2O. In fact, the degradation mechanism of $C_xH_yO_z$ to CO_2 and H_2O is very complex, which we will discuss further on. The chemical reactions at electrodes are simply described by the following equations:

Hongbing Ji

Prof. Hongbing Ji is a professor in School of Chemistry and Chemical Engineering at Sun Sat-Sen University. He received his PhD in the Department of Chemical Engineering from South China University of Technology in 1997. After completing his PhD, he was a lecturer (1997), associate professor (2003) and professor (2006) at South China University of Technology. He carried out his postdoctoral research at Osaka University in Japan from 2000–2002. His research focuses on catalysis and electrochemistry. He has authored 3 books, 222 refereed research publications, 59 patents, and over 120 proceedings and conference articles.

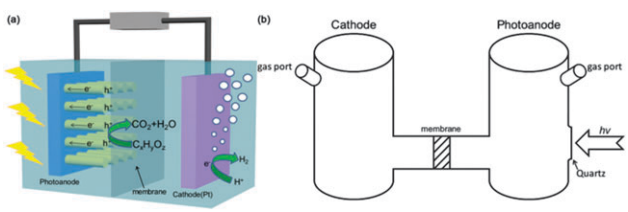

Fig. 2 Schematic diagram of (a) the basic operation mechanism for hydrogen generation from biomass-derived oxygenates ($C_xH_yO_z$) and water, and (b) a typical PEC cell.

$$\text{Photoanode: } TiO_2 + h\nu \rightarrow TiO_2^* + e^- + h^+ \quad (1)$$

$$C_xH_yO_z + (4x + y - 2z)h^+ + (4x + y - 2z)OH^- \rightarrow xCO_2 + (2x + y - z)H_2O \quad (2)$$

$$\text{Cathode: } 2H_2O + 2e^- \rightarrow H_2 + 2OH^- \quad (3)$$

$$\text{Total: } C_xH_yO_z + (2x - z)H_2O \rightarrow xCO_2 + (2x - z + (y/2))H_2 \quad (4)$$

The rates of H_2 production and biomass derivative decomposition strongly depend on the properties of the photoanode, which we will discuss in the following text. Besides the photoanode, the configuration of the PEC reactor also has great influence on the rates of H_2 production and biomass derivative decomposition. A reasonable configuration of the PEC reactor can not only attain the maximum benefit from the irradiation pattern, but also reduce charge recombination phenomena, and hence result in a significant PEC improvement. Fig. 2b show a simple schematic of an H-type PEC reactor. The configuration of this kind of PEC reactor is quite simple, which consists of two vertical glass tubes that are connected by a smaller horizontal tube, a membrane and a flat quartz window to facilitate illumination of the photoelectrode surface.[4,9–11] The connection allows the ion to move between the two compartments, and the gases generated on the anode and cathode will be separated naturally. Additional voltage or bias is usually required to apply to the PEC reactor to either reduce the electron–hole recombination rate or help hydrogen evolve if the photoanode is not energetic enough for water splitting. In order to increase the photo-conversion, a two-compartment PEC cell driven by chemical bias was developed for water splitting recently.[12] This kind of the PEC cell was separated into two compartments by a Nafion membrane, and the photoanode (TiO_2) and cathode (Pt) were immersed in alkaline electrolytes such as KOH and acid electrolytes such as H_2SO_4, respectively. A chemical bias produced by two different electrolytes of different pH values could promote the electron transfer from the photoanode into the cathode rapidly, and the rate of H_2 production will be enhanced. Each unit pH difference between the electrolytes chambers provides 0.06 V, and hence a larger pH difference between the photoanode chamber and cathode chamber is more efficient. In addition, integrating the PEC reactor with a PV cell or dye sensitized solar cell has also proven to enhance the rate of H_2 production. However, there are few reports on the design of a PEC reactor for hydrogen production from biomass derivatives, and until recently, a two-compartment PEC system driven by sunlight and chemical bias was developed to product hydrogen from glycerol and water.[12] The PEC reactors for hydrogen production from biomass derivatives need further study.

3. Photoactive materials for PEC hydrogen from biomass derivatives and water

An ideal photoanode for efficient hydrogen production from biomass derivatives and water should fulfil the following requirements:

(1) suitable band edge positions that straddle reduction potential of water and biomass derivatives;
(2) strong (visible) light harvesting ability;
(3) efficient charge transport in the semiconductor;
(4) excellent chemical and photoelectrochemical stability;
(5) low overpotentials for the reduction–oxidation reactions;
(6) low cost and abundance.

To achieve efficient hydrogen production from biomass derivatives and water, the bottom of the conduction band (CB) of the photoanode should be more negative than the reduction potential of H^+/H_2 (0 V *vs.* NHE at pH = 0), while the top of the valence band (VB) should be more positive than the corresponding biomass derivatives. Fig. 3 shows the band-edge positions of various semiconductors, along with the redox potentials of water and some biomass-derivatives. It is noted that the redox potentials of the biomass derivatives such as methanol, ethanol and glucose are much more negative than that of water, which indicates that these biomass derivatives are more easily oxidized than water by the photoexcited h^+ in the VB of the photoanode.[13] Taking into account the unavoidable energy losses, this potential difference is too weak to make the PEC cell run spontaneously. There is a minimum band gap energy requirement for the photoanode for PEC hydrogen from biomass derivatives and water, which is determined by the energy demand for redox of the reactants,

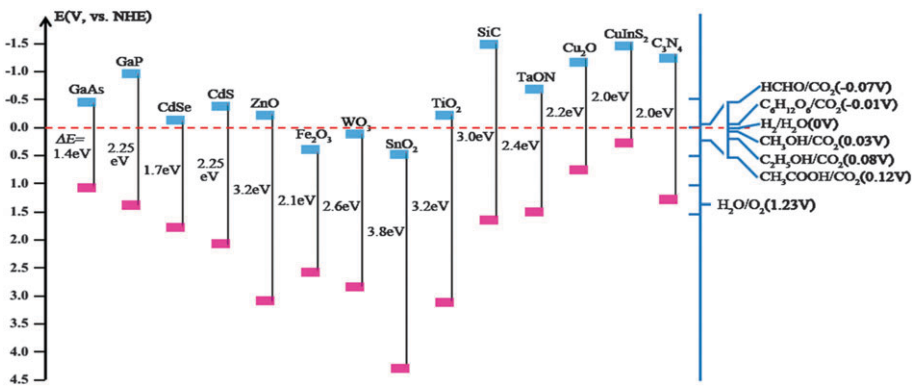

Fig. 3 E_g values (in eV) and position of CB (blue) and VB (pink) for various semiconductors at pH = 0 *vs.* NHE. The diagram was adapted using data from previous publications.[2,23]

the thermodynamic losses and overpotentials. As a result, an external voltage is usually applied that is over the minimum band gap energy, leading to an increase of the electromotive force driving e^- from the photoanode to the photocathode.

Besides the suitable band edge positions, an ideal photoanode for efficient hydrogen production from biomass derivatives and water should have strong light harvesting ability, efficient charge transport, good chemical stability and low cost. Unfortunately, there has been no such photoactive material developed so far that can meet all the above requirements simultaneously. Among the various semiconductors, metal oxides are emerging as the most promising candidates as photoanodes for hydrogen production from biomass derivatives and water, since they are inexpensive, environmental friendly and have a better chemical and photochemical stability. In this regard, various metal oxides such as TiO_2,[9,14–17] WO_3,[18,19] and α-Fe_2O_3 (ref. 20–22) have been extensively investigated as photoanode materials for PEC hydrogen evolution from biomass derivatives and water. However, their intrinsic limitations severely limit their practical application in PEC hydrogen production. For example, TiO_2 (3.0–3.2 eV) has suitable band edge positions which can straddle the electrochemical potentials of E° (H^+/H_2) and E° (O_2/H_2O), while the large band gap limits the utilization of solar light and results in a low solar to hydrogen (STH) conversion efficiency.[21] By contrast, WO_3 has a small band gap of 2.6 eV, which could theoretically utilize ~12% solar light. However, its CB is not negative enough for the reduction of water, and a bias voltage needs to be applied to the WO_3 photoanode in order to evolve hydrogen. Additionally, it can be dissolved in a basic solution and a relatively thick film is required for harvesting light since it is an indirect band-gap semiconductor.[18] Fe_2O_3 has a smaller band gap of 2.1 eV, which can observe longer wavelength and efficiently use the solar spectrum. However, one of the major challenges is that the CB edge position is far away from the E° (H^+/H_2), and a large external bias is also needs to be applied to drive solar water splitting.[22] In order to address these limitations, a lot of effort has been devoted to this work in the past decades, and great progress has been achieved. In the following text, we will review the recent development of TiO_2, WO_3 and Fe_2O_3 as photoanodes for PEC hydrogen production from biomass derivatives and water.

The first development we discuss is the enhancement of the (visible) light harvesting ability by elemental doping and/or sensitization with small band gap semiconductors.[20,24] For instance, Hoang *et al.* reported nitrogen doped TiO_2 nanowires for PEC water oxidation.[24] Due to the introduced N impurity states in the band structure, the pristine white TiO_2 becomes light yellow and IPCE studies show that nitrogen doped TiO_2 exhibited obvious photoactivity in the visible region from 400 to 500 nm. Beside element doping, small band gap semiconductor sensitization, such as CdS,[12] is an alternative method to increase visible light photoactivity of metal oxides. CdS quantum dots are not suitable for direct PEC water splitting, but are suitable for hydrogen production from biomass derivatives and water. This is because the biomass derivatives serve as hole scavengers to consume photoexcited h^+, and hence stabilize these quantum dots. Antoniadou and his co-workers prepared a CdS sensitized TiO_2 photoanode and studied its performance in hydrogen evolution from some biomass derivatives.[12] The CdS/TiO_2 electrode exhibited good visible light photoactivity and excellent stability without observing any CdS photodegradation.

The second strategy is to develop a nanostructured electrode for effective separation and transportation of photoexcited charge carriers.[16,25] In comparison with the bulk structure, the nanostructure could provide greater surface contact with the electrolyte and a shorter diffusion distance for photogenerated minority carriers. Various nanostructures such as nanoparticles, nanowire arrays (NWAs), nanotube arrays (NTAs) and nanoflakes, have been developed and employed as photoanodes for water splitting and biomass derivative decomposition.[3] For instance, Wang *et al.* reported the PEC water splitting and urea oxidation of rutile TiO_2 NWAs on F-doped SnO_2 (FTO) glass.[16] The photocurrent onset potential for films was observed at *ca.* +0.1 V and the photocurrent density at ~1.9 mA cm^{-2}, while the IPCE under monochromatic 400 nm irradiation were found to be 36%. Similarly, a number of efforts have focused on the development of α-Fe_2O_3 nanostructures and the modification of their electronic structure *via* elemental doping. For instance, Zhang *et al.* reported the synthesis of Ti-doped α-Fe_2O_3 electrode by atmospheric pressure chemical vapor deposition (APCVD) and their implementation as photoanodes for glucose oxidation.[20] The introduction of less than 1% of Ti into α-Fe_2O_3 significantly shifted the onset potential to be more negative with a much higher net photocurrent at the same applied bias while the un-doped α-Fe_2O_3 thin films show almost no PEC activity under illumination. Except for these achievements, oxygen evolution reaction (OER) catalysts such as cobalt–phosphate (Co–Pi), $Ni(OH)_2$ have been developed to reduce the over-potential of hematite photoanodes for water oxidation.[22,26] Zhong *et al.* reported that a 5-fold enhancement of the photocurrent density and O_2 evolution rate was observed at +1.0 V *vs.* RHE with the Co–Pi–α-Fe_2O_3 composite photoanodes compared to α-Fe_2O_3 photoanodes.[26]

4. PEC hydrogen production from biomass derivatives and water

Over the past few decades, PEC hydrogen production from biomass derivatives and water has attracted great attention. A huge array of biomass derivatives including alcohols, saccharides and organic acids have been widely explored and used in PEC hydrogen production.[5,16,17,27–30] In this chapter, we will review the recent progress of PEC hydrogen production from simple alcohols (methanol and ethanol), glycerol, saccharides in the presence of water.

4.1 Methanol

In comparison with hydrogen production from water splitting, the processes involved in biomass conversion, in particular concerning methanol, can take place at much lower temperature, at smaller scale, and with easy separation of the gaseous product. As the most simple alcohol, methanol, containing the characteristic CH_2OH unit, which is present in most biomass-derived oxygenates, has been widely used as a resource to

produce hydrogen. Plenty of studies have focused on the investigation of the reaction mechanism of methanol oxidation under light irradiation.[31] The main products after solar driven methanol oxidation are CO_2 and H_2, and its intermediates are formaldehyde and/or formic acid.

The oxidation routes of methanol in different pH solutions are different.[27,31] In neutral or acidic solution, the number of hydroxyl ions (OH^-) is very low, methanol and its intermediates, *i.e.* formaldehyde and formic acid, will directly interact with photogenerated h^+ in the VB of the photoanode to form CO_2 *via* the processes in eqn (6)–(10). In alkaline solution, the number of OH^- is relatively large, which is a well-known efficient hole scavenger, thus h^+ may firstly react with OH^- to generate hydroxyl radicals ($OH^\bullet$), and then the $OH^\bullet$ will react further with the methanol and its intermediate molecules. The interactions at the photoanode (TiO_2) and cathode in neutral, acidic and alkaline solution are described as follow.

(1) Interactions at the photoanode (TiO_2) and cathode in neutral or acidic media:

$$\text{Photoanode: } TiO_2 + h\nu \rightarrow TiO_2^* + e^- + h^+ \quad (5)$$

$$CH_3OH + 2h^+ \rightarrow HCHO + 2H^+ \quad (6)$$

$$HCHO + H_2O + 2h^+ \rightarrow HCOOH + 2H^+ \quad (7)$$

$$HCOOH + 2h^+ \rightarrow CO_2 + 2H^+ \quad (8)$$

$$\text{Cathode: } 2H^+ + 2e^- \rightarrow H_2 \quad (9)$$

$$\text{Total: } CH_3OH + H_2O \rightarrow 3H_2 + CO_2 \quad (10)$$

(2) Interactions at the photoanode and cathode in basic media:

$$\text{Photoanode: } TiO_2 + h\nu \rightarrow TiO_2^* + e^- + h^+ \quad (11)$$

$$6OH^- + 6h^+ \rightarrow 6OH^\bullet \quad (12)$$

$$CH_3OH + 6OH^\bullet \rightarrow CO_2 + 5H_2O \quad (13)$$

$$\text{Cathode: } 2H_2O + 2e^- \rightarrow 2OH^- + H_2 \quad (14)$$

$$\text{Total: } CH_3OH + H_2O \rightarrow 3H_2 + CO_2 \quad (15)$$

It should be pointed out that there are also other possible routes, not included in the above reactions. For instance, other than OH^-, the photogenerated h^+ might react with CH_3OH, producing the reactive intermediate ($CH_2OH^\bullet$, CH_2O, HCOOH, $HCOO^\bullet$, *etc.*).[15]

Hydrogen production from methanol and water through the PC process has been widely investigated and well summarized in the literature, and this system has been frequently used to examine the performance of the photocatalysts.[3] Recently, the PEC process has been intensively explored to produce hydrogen from a methanol and water system.[14,15,27,28] Zhang *et al.* prepared highly ordered TiO_2 NTAs and studied their PEC oxidation behaviour of methanol in PEC hydrogen evolution from a methanol–Na_2SO_4 solution.[28] The adsorbed methanol molecules serve as hole scavengers to react with the h^+ produced in the VB of TiO_2 NTAs, and hence promotes the separation of electron–hole pairs. Mohapatra *et al.* also found that the maximum photocurrent density obtained from a TiO_2 photoanode in 1 M KOH solution was 0.87 mA cm^{-2} while the photocurrent density would increase to 2.43 mA cm^{-2} and the open circuit potential move to −1.02 V *vs.* Ag/AgCl after adding 5 vol% methanol in 1 M KOH solution.[14]

The addition of a noble metal could effectively enhance the separation of the photoexcited electron–hole pairs. On the other hand, some reports also stated that good catalytic activity can be obtained on account of a so-called "support effect" or "cooperative effect". Jia *et al.* presented a simple approach for the fabrication of novel nanoporous gold/TiO_2 (NPG/TiO_2) electrode materials and it showed remarkable performance of methanol photoelectrocatalytic reactions.[15] This noteworthy enhancement can be greatly ascribed to the mediating role of NPG and the photogenerated reactive intermediates which could effectively release the deactivation of NPG.

Considering that the UV region possesses less than 5% of the total solar energy, it is more ideal in the case of photoanodes with a band gap smaller than 3 eV in practical application. Recently, the potentiostatic anodization of metallic tungsten has been investigated by Cristino *et al.* in order to improve the PEC activity of the WO_3 layer for water oxidation.[32] In the presence of an electrolyte composed of 1 M H_2SO_4/CH_3OH = 8 : 2, the plateau photocurrents are nearly doubled and approach 16 mA cm^{-2} under strong illumination (*ca.* 0.3 W cm^{-2}). Furthermore, the rectangular shape of the shuttered *J*–*V* transient curves in Fig. 4 recorded under illumination of *ca.* 0.1 W cm^{-2} can illustrate the effective photo-induced charge separation and transport with the presence of small photo-anodic transients in the immediate proximity of the flat band potential, and the lack of cathodic features in the presence of methanol, acting as a hole scavenger. This increase in photocurrent may be partially attributed to improved kinetics for the methanol oxidation reaction compared to the OER, but also to photocurrent multiplication. Besides TiO_2 and WO_3, other metal oxides such as CeO_2 (ref. 33) and In_2O_3 (ref. 34) have also been used as photoanodes for hydrogen production from PEC methanol oxidation.

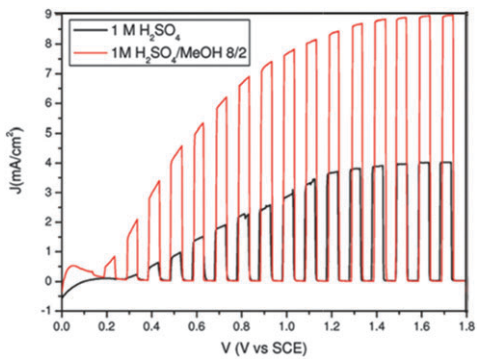

Fig. 4 Shuttered *J*–*V* curves in 1 M H_2SO_4 (black) and 1 M H_2SO_4/CH_3OH = 8 : 2 (red). The incident irradiance is 0.120 W cm^{-2}. Reprint with permission from ref. 32 permission from American Chemical Society.

4.2 Ethanol

Ethanol, produced from conventional fermentation of sugars and starch, is one of the most attractive renewable hydrogen sources because it is globally available and easy to transport, biodegradable, and has low-toxicity. Hydrogen production from PC/PEC ethanol reforming has been studied for several decades; this process is not only effective and environmentally friendly, but also opens a new opportunity for the low cost utilization of this renewable resource.[6]

A lot of studies have been devoted to PEC hydrogen production from ethanol and water.[30,35,36] The route of ethanol oxidation is similar to the route of methanol but there are some differences. One of the differences between methanol and ethanol is that a lot of acetaldehyde will be produced, especially at the early stage of irradiation.[36] During the oxidation of ethanol, the formed acetaldehyde can go through two alternative routes. One of them leads to acetic acid formation, limits hydrogen but favors methane production. In the other one ethanol decomposes into CO_2 thoroughly. But some reports demonstrated that the reaction will be mostly favoured in the presence of oxygen.[37] The reactions at the TiO_2 photoanode and cathode in neutral, acidic and alkaline solution are proposed as follow.

(1) Interactions at the photoanode (TiO_2) and cathode in neutral or acidic media:

$$\text{Photoanode: } TiO_2 + h\nu \rightarrow TiO_2^* + e^- + h^+ \quad (16)$$

$$C_2H_5OH + 2h^+ \rightarrow CH_3CHO + 2H^+ \quad (17)$$

$$CH_3CHO + H_2O + 2h^+ \rightarrow CH_3COOH + 2H^+ \quad (18)$$

$$CH_3COOH \rightarrow CO_2 + CH_4 \quad (19)$$

$$CH_3CHO + 3H_2O + 10h^+ \rightarrow 2CO_2 + 10H^+ \quad (20)$$

$$\text{Cathode: } 2H^+ + 2e^- \rightarrow H_2 \quad (21)$$

$$\text{Total: } C_2H_5OH + 3H_2O \rightarrow 6H_2 + 2CO_2 \quad (22)$$

$$C_2H_5OH + H_2O \rightarrow 2H_2 + CO_2 + CH_4 \quad (23)$$

(2) Interactions at the photoanode and cathode in basic media:

$$\text{Photoanode: } TiO_2 + h\nu \rightarrow TiO_2^* + e^- + h^+ \quad (24)$$

$$12OH^- + 12h^+ \rightarrow 12OH^\bullet \quad (25)$$

$$C_2H_5OH + 12OH^\bullet \rightarrow 2CO_2 + 9H_2O \quad (26)$$

$$\text{Cathode: } 2H_2O + 2e^- \rightarrow 2OH^- + H_2 \quad (27)$$

$$\text{Total: } C_2H_5OH + 3H_2O \rightarrow 6H_2 + 2CO_2 \quad (28)$$

Antoniadou *et al.* studied the photooxidation behaviour of ethanol over a nanocrystalline TiO_2 electrode in a two-compartment chemically biased cell.[30] The electrolyte of the anode compartment contained NaOH and that of the cathode contained H_2SO_4 at various concentrations. The two compartment cell with different NaOH and H_2SO_4 concentrations could provide a chemical bias between 637 mV and 732 mV. The open-circuit potential (OCP) shifted to a more negative position after adding ethanol in the anode compartment, and the presence of ethanol dramatically enhanced the photocurrent density, as shown in Fig. 5a. By studying the influence of the ethanol concentration, it is found that the maximum current was obtained in the presence of 20% ethanol, however, the current was only 10% lower when the concentration was ten times lower (*i.e.* 2%). This behaviour can be explained by the fact that decomposition of small quantities of ethanol at the TiO_2 photoanode was very efficient but reached saturation when the quantity of ethanol became relatively large. Fig. 5b gives the hydrogen production rate and the corresponding photocurrent density in the presence of ethanol. The quantity of expected hydrogen molecules per unit of time in the presence of ethanol, for I = 8.9 mA, is 2.8×10^{16} hydrogen molecules per second. The actual measured number, for a rate of 2.25 mmol H_2 per min, was 2.3×10^{16} hydrogen molecules per second, *i.e.* 82% of the expected. The performance of TiO_2 photoanode could be further improved by increasing the thickness of TiO_2 layer.[29]

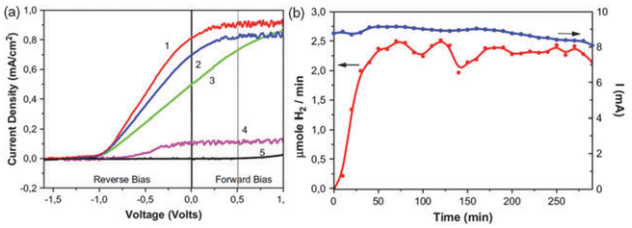

Fig. 5 (a) Current–voltage characteristics under UVA (black light) illumination of the cell containing the following electrolytes. The first electrolyte corresponds to the anode compartment and the second to the cathode compartment: (1) 1 M NaOH + 20 vol% ethanol *vs.* 1 M H_2SO_4; (2) 1 M NaOH + 20 vol% ethanol *vs.* 0.5 M H_2SO_4; (3) 0.5 M NaOH + 20 vol% ethanol *vs.* 0.1 M H_2SO_4; (4) 1 M NaOH (no ethanol) *vs.* 1 M H_2SO_4; and (5) dark current (b) current intensity (upper curve) and hydrogen production rate (lower curve) in a two-compartment PEC cell containing 1 M NaOH + 20 vol% ethanol in the anode compartment and 1 M H_2SO_4 in the cathode compartment. Reprinted from ref. 30 with permission from the International Association of Hydrogen Energy.

To understand further the nature of the effect of alcohols and some other organic compounds on the photocatalytic efficiency of various types of TiO_2 photocatalysts, Semenikhin *et al.* demonstrated that the addition of a model organic compound, ethanol, resulted in the virtual suppression of surface recombination on anatase TiO_2 photoelectrodes by using IMPS.[38] Comparison of the frequency spectra of modulated photocurrents obtained with and without ethanol in the solution, shows that ethanol can effectively suppress surface recombination over a wide potential range near the flat band potential. Such behaviour is believed to be the main reason for the high catalytic activity of anatase TiO_2 in the photodecomposition of organic pollutants. Zhou *et al.* doped TiO_2 with non-metallic elements, carbon, and introduced trapping sites to prevent the rapid recombination of h^+ and e^-, thus improving the catalytic activity.[35] They also found that the current increased with the increased concentration, which is in accordance with results reported by Antoniadou.[29]

WO_3 is also used as a visible light driven photoanode for hydrogen production from ethanol and water. Barczuk *et al.* developed a visible light-driven photoanode for PEC conversion

of the ethanol and its by-product by using a mesoporous WO_3 film.[39] The IPCE of the mesoporous WO_3 photoanode in ethanol solution are largely over 100%.

4.3 Glycerol

Glycerol, an important organic industry and medical material, is extensively used in organic synthesis and in the pharmaceutical industry. Additionally, it is a by-product of the biodiesel-making process. As a result, large amounts of glycerol often occur in wastewater from this industry. This wastewater can cause eutrophication of the water-body and result in the shortage of oxygen and the death of organisms in the water-body. New applications of glycerol as a low-cost feedstock should be developed to make biodiesel production more profitable and sustainable. Previous studies and efforts on catalytic conversion of glycerol have been described extensively, especially when converting glycerol to H_2 and advanced achievements have been made.[40] The mechanisms for PEC glycerol reforming are similar to those of ethanol, but more complicated. It still needs more analysis and evaluation of the intermediates.

In addition to the PC process, the PEC process was also developed to produce hydrogen from glycerol. Mohapatra *et al.* prepared TiO_2 NTAs on Ti foil by an anodization method and studied their PEC behaviour as photoanodes in the presence of methanol, ethylene glycol and glycerol.[14] A high charge carrier density and reduction of recombination losses were observed in the organically modified electrolytes as compared to that in aqueous basic solution. As shown in Fig. 6, the open circuit potential (OCP) of the TiO_2 NTAs photoanode moved to −1.26 V (*vs.* Ag/AgCl) and achieved a photocurrent density of 2.55 mA cm^{-2} at 0.2 V (*vs.* Ag/AgCl) in the glycerol solution, which is substantially higher than that in 1 M KOH solution and methanol solution. On the other hand, other hydroxyl organic additives, such as ethanol, isobutyl alcohol, and sucrose were also studied, and similar results were obtained.

Several attempts are reported to improve the PEC activity of the TiO_2 photoanode toward glycerol reforming.[12] Oxygen vacancies are known to be shallow donors for TiO_2, with relatively low formation energies and have proven to play a critical role in determining the surface and electronic properties of TiO_2.[41] A composite photoanode consisting of CdS

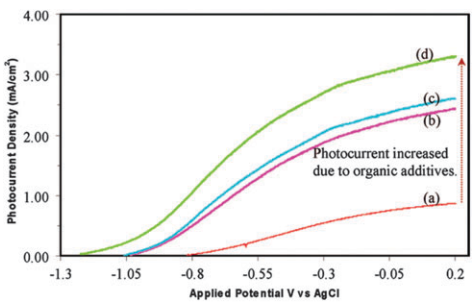

Fig. 6 LSW curves of TiO_2 NTAs photoanode in 1 M KOH solution containing (a) without organic additives (b) 5% methanol, (c) 5% glycerol and (d) 5% ethylene glycol as organic additive. Reprinted from ref. 14 with permission from the American Chemical Society.

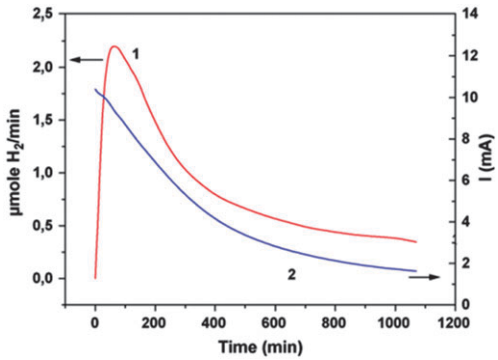

Fig. 7 (a) Hydrogen evolution rate (1) and short-circuit current (2) as a function of time for a cell bearing a TiO_2/FTO photoanode, run under UVA illumination and containing the following electrolytes: 1 M NaOH + 20% *vs.* glycerol *vs.* 1 M H_2SO_4. Reprinted from ref. 12 with permission from Elsevier.

and TiO_2 was also prepared and exhibited a good visible light activity for PEC glycerol reforming.[12]

Palmas *et al.* studied the redox behaviour of glycerol at TiO_2 electrodes under light irradiation,[25] and found that the glycerol was strongly absorbable at defects and this can be usefully exploited in order to obtain the oxidation of the molecule. On the other hand, when the concentration of defects is rather high, the adsorbed glycerol can react directly with the photo-generated h^+ in the system, while conversely its indirect reduction seems to proceed *via* H incorporated in the lattice.

In view of addressing the practical application of this system, Antoniadou *et al.* developed a two-compartment, chemically biased PEC to produce hydrogen from glycerol.[12] The PEC cell was a H-shaped reactor made of Pyrex glass. The photoanode was made of one single FTO glass with deposited nanocrystalline TiO_2, while the cathode was Pt nanoparticles. The electrolyte of the anode compartment contained 1 M NaOH and that of the cathode contained 1 M H_2SO_4, which provides a chemical bias to promote glycerol oxidation. Fig. 7 shows the proportional hydrogen evolution in the case of glycerol together with the value of photocurrent. Both the current and the hydrogen production rate decreased in the course of time. Several reasons should be responsible for this decrease. The first one is the consumption of the initial glycerol. However, the time is not enough to mineralize the glycerol completely after several hours of illumination. The second one may be the decrease of the chemical bias, which was caused by the exchange of cations through the Nafion membrane and the small increase of the pH. The deterioration of the electrode could also influence the efficiency and a fresh cathode improves efficiency by about 10%. However, the main reason for this sharp decrease should be further investigated.

4.4 Saccharides

Saccharides $(C_6H_{12}O_6)_n$ such as glucose (n = 1), saccharose (n = 2), starch ($n \approx 100$), cellulose ($n \approx 1000$ to 5000) have been proposed and examined as an alternative and potential hydrogen feedstock since they are abundant, cheap, renewable and easy to obtain.[5,19,42] Saccharides are one of the main

products of photosynthesis and are widely present in nature. On the other hand, they are one of the main wastes in agricultural, foods and pulp industries in the world, which could raise serious environmental pollution when not dealt with well. As a result, the development of new technology to convert saccharides into useful chemicals has attracted much attention. One of the reasonable ways is to utilize them for the sustainable production of hydrogen and some achievements have been made, for example, steam gasification, fast pyrolysis, and supercritical conversion.[43] Unfortunately, these processes are not economic because they all require rigorous conditions, such as high temperature or high pressure. The pioneer study, conducted in 1980 by Kawai *et al.* reported that hydrogen could be generated from the saccharose, starch and cellulose over the $RuO_2/TiO_2/Pt$ photocatalyst under UV light irradiation.[7] A lot of attention has been paid to PC hydrogen production from saccharides, and multifarious saccharides including glucose, saccharose and starch which have been widely explored in PC hydrogen production.

Among various saccharides, glucose, also known as D-glucose, is a simple monosaccharide found in plants and one of the main products in photosynthesis. Over the past few decades, great efforts have been devoted to PC/PEC hydrogen production from glucose. John *et al.* studied the photocatalytic reaction of glucose over Pt/TiO_2 in aqueous solution.[44] The TiO_2 electrodes in glucose solution exhibited a more negative flat-band potential of about 210 mV than that without glucose. Fu *et al.* examined the effect of several noble metals on anatase TiO_2 on the PC hydrogen production, and found that the hydrogen evolution rates are decreased in the order Pd > Pt > Au ≈ Rh > Ag ≈ Ru.[42] A possible mechanism of PC/PEC reforming glucose to hydrogen is proposed. Firstly, a glucose (denoted as RCH_2OH) molecule prefers to bond with under coordinated surface Ti atoms through its hydroxyl O. Then, the hydroxyl group dissociates to H^+ and $RCH_2–O^-$, following by $RCH_2–O^-$ trapping a h^+ and itself oxidization to $RCH_2–O^\bullet$ radical.

$$TiO_2 + h\nu \rightarrow TiO_2^* + e^- + h^+ \quad (29)$$

$$h^+ + H_2O \rightarrow {}^\bullet OH + H^+ \quad (30)$$

$$RCH_2OH \rightarrow H^+ + RCH_2–O^- \quad (31)$$

$$RCH_2–O^- + h^+ \rightarrow RCH_2O^\bullet \quad (32)$$

This $RCH_2–O^\bullet$ radical will attack another glucose (denoted as $R'CH_2OH$) molecule and the radical electron transfers to the C atom of the latter, and then generates a $R'CH_2OH$ radical. $R'CH_2OH$ continues deprotonating subsequently to form $R'CHO$ by repeating the process. The $R'CHO$ was further oxidized by the surface-bound hydroxyl radical, transferring to $[R'COOH]^-$.

$$RCH_2O^\bullet + R'CH_2OH \rightarrow {}^\bullet CH(R')OH + RCH_2OH \quad (33)$$

$$^\bullet CH(R')OH + h^+ \rightarrow H^+ + {}^\bullet CH(R')O^\bullet \quad (34)$$

$$^\bullet CH(R')O^\bullet \rightarrow R'CHO \quad (35)$$

$$R'CHO + {}^\bullet OH \rightarrow [R'COOH]^- + H^+ \quad (36)$$

Finally, $[R'COOH]^-$ decarboxylated *via* a photo-Kolbe reaction resulting in eventual CO_2.[37]

$$[R'COOH]^- + h^+ \rightarrow R'H + CO_2 \quad (37)$$

During the reaction, the H_2 deprotonated from glucose in the whole process will transfer to the loaded Pt particles (Pt cathode) and then is reduced to H_2 by photogenerated e^-. Q7

$$2H^+ + e^- \rightarrow H_2 \quad (38)$$

To further understand the mechanism of PC/PEC reforming from glucose, Du *et al.* also studied the photooxidation of glucose ($C_6H_{12}O_6$) on the (101) surface of anatase TiO_2 by first-principles calculations based on density functional theory with the generalized gradient correction and the projector augmented wave method.[45] They also revealed the microscopic mechanisms for the separation and transfer of photogenerated e^- and h^+ at the TiO_2–molecule interface as detailed from hole trapping, deprotonation, to the formation of an electron–hole recombination centre. Interestingly, it is found that only dissociatively adsorbed glucoses induce occupied electronic states inside the TiO_2 band gap, whereas molecularly adsorbed ones do not. The glucose unit will undergo photochemical reactions that transfer the positive charges carried by the h^+ to those of the dissociated protons, H^+, bound on nearby surface O ions. These protons cannot easily diffuse into the surrounding bulk water, because the calculation shows that an H_3O^+ ion will spontaneously dissociate into an H_2O molecule and a surface-bound H^+. The surface hopping of the H^+ to O sites distant away from the glucose is also inhibited due to a Coulomb attraction by the negatively charged glucose. In addition, the reduction of H^+ by photoelectrons in TiO_2 to form H_2 molecules cannot happen in the absence of a metal catalyst. The trapping of the h^+ by the molecularly adsorbed glucose should be much slower than that by the dissociatively adsorbed one due to the lack of gap states. Therefore, the abundance of hydroxyls in sugars leads to easier activation of the substrate, though the full degradation of their complex structure is much more complex than simple alcohols. Thus, lower productivity is usually observed.

Noble metal–TiO_2 hybrid systems have been extensively explored for PC and PEC reforming of glucose, and have proven to have a better performance than pristine TiO_2.[46,47] This kind of nanocomposite not only retains the catalytic activity of metal nanoparticles (NPs) but also possesses the intrinsic photocatalytic capacity of TiO_2. Wen *et al.* have prepared a novel metal–semiconductor hybrid nanostructure with enhanced catalytic functions by a simple self-assembly approach.[46] This new bifunctional nanocatalyst consists of evenly dispersed Au–Pt hybrid NPs (Au–Pt NPs) assembled on NH_2 group functionalized anatase TiO_2 colloid spheres with a nanoporous surface (f-TiO_2). Compared with the f-TiO_2, the PEC results indicate that the as-prepared f-TiO_2–Au/Pt NPs exhibited a more prominent photocatalytic property toward glucose oxidation. Gan *et al.* studied the PC and PEC oxidation of glucose over TiO_2 and Pt/TiO_2 electrodes under similar conditions.[47] The overall oxidation efficiency of the PEC process was found to be better than the PC process, for both TiO_2 and Pt/TiO_2 films. Additionally, the Pt/TiO_2

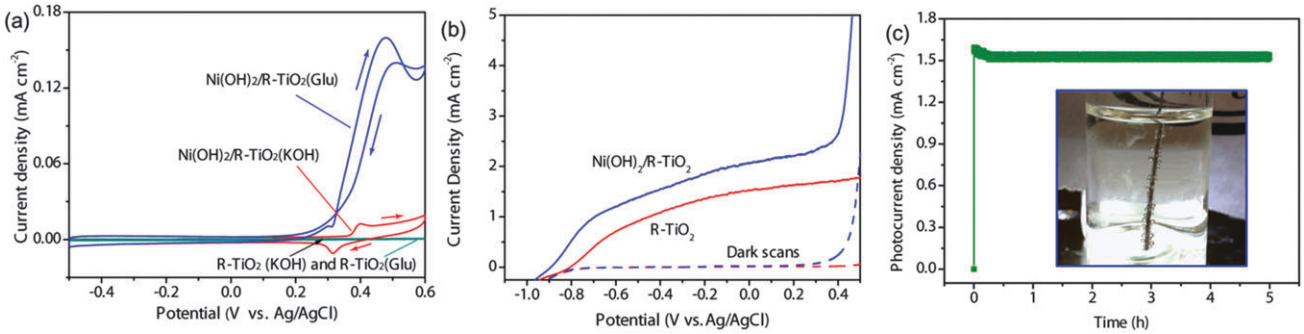

Fig. 8 (a) CV curves collected for R-TiO_2 and $Ni(OH)_2$/R-TiO_2 electrodes at a scan rate of 10 mV s^{-1} in a 1 M KOH aqueous solution without/with 0.1 M glucose. The direction of the arrow indicates the scan direction. (b) LSW curves collected for R-TiO_2 (red) and $Ni(OH)_2$/R-TiO_2 (blue) electrodes in the dark (dashed lines) and under light illumination (100 mW cm^{-2}). (c) Photocurrent–time response curve of the $Ni(OH)_2$/R-TiO_2 electrode collected at −0.3 V *vs.* Ag/AgCl in a 1 M KOH aqueous solution with 0.1 M glucose. Inset: photoimage of Pt wire collected at −0.3 V in a 1 M KOH aqueous solution with 0.1 M glucose. Reprinted from ref. 17.

electrode exhibited higher PEC glucose oxidation efficiency than the pristine TiO_2 electrode at an applied cathodic potential bias. However, the use of noble metals leads to high cost, which seriously restricts their practical application.

Recently, Xie *et al.* demonstrated that efficient hydrogen production from glucose solution was achieved over a novel $Ni(OH)_2$ functionalized electro-reduced TiO_2 (denoted $Ni(OH)_2$/R-TiO_2) photoanode.[17] Fig. 8a is the CV curves of R-TiO_2 and $Ni(OH)_2$/R-TiO_2 NWAs at 10 mV s^{-1} without/with 0.1 M glucose. Significantly, the $Ni(OH)_2$/R-TiO_2 electrode exhibits well-defined redox peaks in the potential range between 0.3 and 0.4 V *vs.* Ag/AgCl in a 1 M KOH aqueous solution without/with 0.1 M glucose. This redox peak can be attributed to the Ni^{2+}–Ni^{3+} transition.[16] Moreover, the $Ni(OH)_2$/R-TiO_2 electrode shows a significantly enhanced current at the potential of 0.3 V *vs.* Ag/AgCl or above in the presence of glucose, revealing that glucose is indeed oxidized at this electrode. In contrast, only a small background current without clear redox peaks is observed for the electro-reduced TiO_2 (R-TiO_2) electrode, which indicates that neither water oxidation nor glucose oxidation occurs in this potential window. On the other hand, the LSW curves of R-TiO_2 and $Ni(OH)_2$/R-TiO_2 electrodes under light irradiation collected in Fig. 8b exhibit a more negative onset potential and higher oxidation current density, indicating that the nano-composite electrode has superior performance for glucose oxidation. Additionally, the $Ni(OH)_2$/R-TiO_2 electrode exhibited good stability for solar driven glucose oxidation. On the other hand, a large number of H_2 gas bubbles are observed at the Pt wire electrode under light illumination at −0.3 V (Fig. 8c). The calculated efficiency of the $Ni(OH)_2$/R-TiO_2 electrode achieves 79% at −0.3 V *vs.* Ag/AgCl after 5 h irradiation.

A bias voltage must be applied to a WO_3 photoanode in order to evolve hydrogen from a PEC cathode. To realize the self-driven hydrogen evolution over a WO_3 photoanode from glucose, Esposito *et al.* recently studied the PEC behaviours of a WO_3 photoanode in the presence of glucose and developed a novel WO_3-based tandem PEC cell.[19] The film WO_3 photoanode exhibits excellent photocatalytic activity towards the oxidation of glucose. After 3 and 10 h of operation at 1.2 V *vs.* SCE in 5 mM and 100 mM glucose solutions under light irradiation, (Fig. 9a), gases evolved from the WO_3 photoanode and O_2, CO, and CO_2 are detected. This indicates that all the C–C bonds in

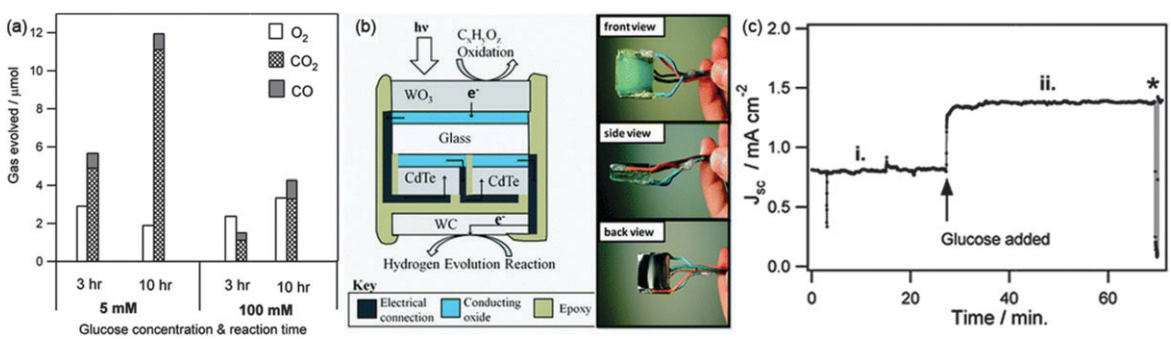

Fig. 9 (a) Amounts of product gases evolved from a WO_3 photoelectrode during chronoamperometry measurements conducted in 5 and 100 mM glucose solutions in deaerated 0.33 M H_2SO_4 supporting electrolyte. Photoelectrodes were held at 1.2 V SCE under constant illumination by a UV-LED light assembly. Gas quantities were determined from GC analysis of gas sampled from the headspace of the enclosed PEC test cell. (b) Schematic side-view of a WO_3|CdTe|WC tandem cell device and photographs of an actual device. External wires attached to each tandem cell component (WO_3, CdTe, WC) allowed for measurement of the current–voltage characteristics of either the whole device or an individual component. (c) Short-circuit current (J_{sc}) recorded for a WO_3|CdTe|WC tandem device under outdoor illumination in (i) 0.33 M H_2SO_4 and (ii) 0.33 M H_2SO_4 + 0.1 M glucose. Reprinted from ref. 19.

glucose can be dissociated by the WO_3 photoanode under the irradiation. In addition, the content of CO_2 and CO is dependent on the glucose concentration. Less CO_2 is detected in the test cell headspace for the 100 mM glucose solution than for the 5 mM solution, and the average extent of conversion in the 5 mM solution after 10 h is significantly higher than that for the 100 mM solution. These findings mean that it is possible to control the product gas composition and makes the WO_3 photoanode suitable for PEC production of either H_2 or syngas through careful selection of the PEC reactor conditions and catalytic modification of the WO_3 surface. Fig. 9b shows the schematic diagram of the fabricated tandem PEC cell device, which consists of a WO_3 photoanode, a CdTe PV cell, and a WC counter electrode. The WO_3|CdTe|WC tandem device exhibits enhanced PEC performance in aqueous solution containing 0.1 M glucose and 0.33 M H_2SO_4. The photocurrent density achieved was 1.38 mA cm^{-2} without any applied bias (Fig. 9c), which is equated to a H_2-production rate of 25.7 mmol H_2 cm^{-2} s^{-1} when assuming the faradaic efficiency of the H_2-evolving counter electrode is 100%.

Hematite (α-Fe_2O_3) is an attractive photoanode material for glucose oxidation and doping hematite with nonmetal elements and metal elements has been demonstrated to be an effective strategy to improve their PEC performance. Zhang *et al.* reported the synthesis of a Ti-doped α-Fe_2O_3 electrode by atmospheric pressure APCVD and their implementation as photoanodes for glucose oxidation.[20] Under the applied bias of 0.2 V *vs.* Ag/AgCl, the IPCE at 400 nm after calcination and surface modification reached 12.5%, and further improved to 15.7% with the presence of glucose. It is noted that the performance only increases slightly in the presence of glucose at 0.4 V *vs.* Ag/AgCl. The results may be the consequence of two factors. One is that the applied potential does not provide sufficient compensation due to the poor oxidizability of α-Fe_2O_3. The other is the high intrinsic recombination rates although the surface recombination is hindered by the glucose. Therefore, there is still scope for further improvement of the photoanodes.

In recent years, Ni based OER catalysts such as nickel hydroxide, nickel oxide and nickel borate have attracted a lot of interest, due to their good catalytic performance, low cost and low toxicity.[22] The further improved performance of the OER or PEC was attributed to the catalytic effect of the Ni catalyst that suppressed the overpotential for water oxidation. Therefore, the PEC performance can largely be promoted if the semiconductors are combined with these Ni based catalysts. Recently, efficient hydrogen evolution from PEC glucose oxidation over $Ni(OH)_2$ functionalized α-Fe_2O_3 (denoted $Ni(OH)_2/Fe_2O_3$) photoanode has been reported by Wang *et al.*[22] Fig. 10 shows the LSV curves of the $Ni(OH)_2/Fe_2O_3$ electrode in the presence and absence of glucose. Significantly, the photocurrent density of the $Ni(OH)_2/Fe_2O_3$ electrode in the presence of glucose is substantially higher (about 2 times) than that without glucose, indicating that glucose could be indeed oxidized by the $Ni(OH)_2/Fe_2O_3$ electrode. The mechanism for PEC glucose oxidation over this $Ni(OH)_2/Fe_2O_3$ electrode is suggested as follows: photoexcited e^- and h^+ are first generated in Fe_2O_3 under light illumination. The Ni^{2+} is oxidized quickly to Ni^{3+} by the photo-excited h^+, resulting in the efficient separation of photoexcited electron–hole pairs. Then, the formed Ni^{3+} acts as catalyst to oxidize glucose. Simultaneously, the e^- transfers to Pt cathode to reduce water to H_2.

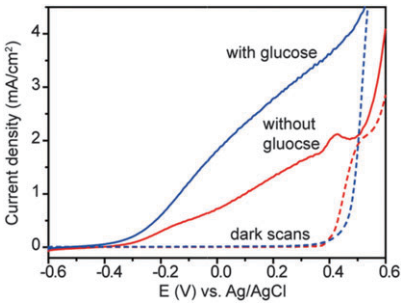

Fig. 10 LSV curves of $Ni(OH)_2/Fe_2O_3$ collected in 1 M KOH solution with/without glucose, in the dark (dashed lines) and light illumination (solid lines; AM 1.5G 100 mW cm^{-2}) at a scan rate of 50 mV s^{-1}. Reprinted from ref. 22.

4.5 Other biomass derivatives

Besides the above-mentioned biomass derivatives, there are some other renewable biomass derivatives, such as formic acid,[27,48] propionic acid, levulinic acid,[49] formaldehyde,[27,48] or apple vinegar.[50] For instance, Seger *et al.*[27] studied hydrogen generation during 24 h of consecutive irradiation obtained from an electrolyte containing 1 M formic acid and 0.1 M sulfuric acid. It holds a constant 150 mA cm^{-2} over the whole time and states a good activity and stable ability of the PEC cell. Moreover, the temperature has a deleterious effect on the open circuit voltage, while it gives a slightly positive effect on the maximum hydrogen production. Highly ordered TiO_2 NTAs was constructed by Gan *et al.*[50] and then studied its photo-reforming of apple vinegar. Interestingly, the results showed that the apple vinegar solution has the highest hydrogen generation rate of around 1.67 per unit volume of biomass solution per second (μL L^{-1} s^{-1}).

5. Conclusion and outlook

Hydrogen production from renewable biomass derivatives and water through a PEC process is an attractive and effective approach because it combines H_2 production with degradation of organic substances from wastewater. The rate of hydrogen production and biomass derivative decomposition strongly depends on the properties of the photoanode. TiO_2, WO_3, and α-Fe_2O_3 have been extensively investigated as photoanodes for PEC hydrogen evolution from biomass derivatives and water due to their good photoactivity, abundance, low cost and environmental friendliness. However, their practical applications are severely limited by their intrinsic limitations. In order to address these problems, various strategies including structural engineering, elemental doping, small band gap semiconductor sensitization, surface modification with catalyst and metal have been developed to improve the performance of these oxide photoanodes. In particularly, coupling of the photoanodes with non-precious metal catalysts such as $Ni(OH)_2$ and Co–Pi have

shown great potential to significantly boost the rate of hydrogen production and biomass derivative degradation. On the other hand, the development of highly active photoanodes driven in the visible light could be the future important research direction since only a few visible-light driven photoanodes have been reported.

Besides photoanodes, the nature of the biomass derivative as well as its concentration also has great influence on the performance for PEC hydrogen production from the biomass derivative and water. For instance, the rate of hydrogen evolved from methanol glycerol and ethylene glycol *via* the same PEC process is clearly distinguished, and the ethylene glycol solution exhibited the fastest rate.[14] This is attributed to the varied oxidation capability and reaction mechanism between different biomass derivatives. A variety of biomass derivatives such as alcohols, saccharides, organic acids and nitrogen compounds have been explored to produce hydrogen in a PEC cell. The possible reaction mechanisms of some biomass derivatives have been proposed in recent years. However, further detailed investigations are still needed to understand the basic step of these reactions, surface interactions between the adsorbent and the adsorbate and the nature of the active species, especially for complex molecules.

In comparison with the photoanode and biomass derivatives, the research on the design of the PEC system is rare. To date, only a few studies have focused on the development of an efficient PEC system for hydrogen production from biomass derivatives and water. Until recently, a two-compartment PEC system driven by sunlight and chemical bias was developed to produce hydrogen from glycerol and water.[12] As a matter of fact, the development of the efficient PEC system to produce hydrogen from biomass derivatives and water is very desirable and necessary for their practical application. It is indeed expected that more efficient and novel PEC systems will occur with the advancement in our ability to synthesize nanomaterials and understand reaction mechanism of biomass derivatives.

Acknowledgements

The authors acknowledge the financial support of this work by the Natural Science Foundations of China (21036009 and 21273290), and the Natural Science Foundations of Guangdong Province (S2013030013474), the Research Fund for the Doctoral Program of Higher Education of China (20120171110043), and the Young Teacher Starting-up Research of Sun Yat-Sen University.

Notes and references

1 L. Fulcheri and Y. Schwob, *Int. J. Hydrogen Energy*, 1995, **20**, 197–202.
2 A. Fujishima and K. Honda, *Nature*, 1972, **238**, 37–38.
3 X. Chen, S. Shen, L. Guo and S. S. Mao, *Chem. Rev.*, 2010, **110**, 6503–6570.
4 C. Ampelli, R. Passalacqua, C. Genovese, S. Perathoner and G. Centi, *Chem. Eng. Trans.*, 2011, **25**, 683–688.
5 J. A. Melero, J. Iglesias and A. Garcia, *Energy Environ. Sci.*, 2012, **5**, 7393–7420.
6 K. Lee, R. Hahn, M. Altomare, E. Selli and P. Schmuki, *Adv. Mater.*, 2013. Q8
7 T. Kawai and T. Sakata, *Nature*, 1980, **286**, 474–476.
8 M. Kawai, T. Kawai and K. Tamaru, *Chem. Lett.*, 1981, 1185–1188.
9 Y. Sun, G. Wang and K. Yan, *Int. J. Hydrogen Energy*, 2011, **36**, 15502–15508.
10 L. J. Minggu, W. R. Wan Daud and M. B. Kassim, *Int. J. Hydrogen Energy*, 2010, **35**, 5233–5244.
11 E. Selli, G. L. Chiarello, E. Quartarone, P. Mustarelli, I. Rossetti and L. Forni, *Chem. Commun.*, 2007, 5022–5024.
12 M. Antoniadou and P. Lianos, *J. Photochem. Photobiol., A*, 2009, **204**, 69–74.
13 Y. Taniguchi, H. Yoneyama and H. Tamura, *Chem. Lett.*, 1983, 269–272.
14 S. K. Mohapatra, K. S. Raja, V. K. Mahajan and M. Misra, *J. Phys. Chem. C*, 2008, **112**, 11007–11012.
15 C. C. Jia, H. M. Yin, H. Y. Ma, R. Y. Wang, X. B. Ge, A. Q. Zhou, X. H. Xu and Y. Ding, *J. Phys. Chem. C*, 2009, **113**, 16138–16143.
16 G. Wang, Y. Ling, X. Lu, H. Wang, F. Qian, Y. Tong and Y. Li, *Energy Environ. Sci.*, 2012, **5**, 8215–8219.
17 S. Xie, T. Zhai, W. Li, M. Yu, C. Liang, J. Gan, X. Lu and Y. Tong, *Green Chem.*, 2013, **15**, 2434–2440.
18 G. Wang, Y. Ling, H. Wang, X. Yang, C. Wang, J. Z. Zhang and Y. Li, *Energy Environ. Sci.*, 2012, **5**, 6180–6187.
19 D. V. Esposito, R. V. Forest, Y. Chang, N. Gaillard, B. E. McCandless, S. Hou, K. H. Lee, R. W. Birkmire and J. G. Chen, *Energy Environ. Sci.*, 2012, **5**, 9091–9099.
20 P. Zhang, A. Kleiman-Shwarsctein, Y.-S. Hu, J. Lefton, S. Sharma, A. J. Forman and E. McFarland, *Energy Environ. Sci.*, 2011, **4**, 1020–1028.
21 G. Wang, Y. Ling and Y. Li, *Nanoscale*, 2012, **4**, 6682–6691.
22 G. Wang, Y. Ling, X. Lu, T. Zhai, F. Qian, Y. Tong and Y. Li, *Nanoscale*, 2013, **5**, 4129–4133.
23 T. Inoue, A. Fujishima, S. Konishi and K. Honda, *Nature*, 1979, **277**, 637–638.
24 S. Hoang, S. Guo, N. T. Hahn, A. J. Bard and C. B. Mullins, *Nano Lett.*, 2011, **12**, 26–32.
25 S. Palmas, A. Da Pozzo, M. Mascia, A. Vacca, P. C. Ricci and R. Matarrese, *J. Solid State Electrochem.*, 2012, **16**, 2493–2502.
26 D. K. Zhong and D. R. Gamelin, *J. Am. Chem. Soc.*, 2010, **132**, 4202–4207.
27 B. Seger, G. Q. M. Lu and L. Wang, *J. Mater. Chem.*, 2012, **22**, 10709–10715.
28 Z. Zhang, Y. Yuan, Y. Fang, L. Liang, H. Ding, G. Shi and L. Jin, *J. Electroanal. Chem.*, 2007, **610**, 179–185.
29 M. Antoniadou, D. Kondarides, D. Labou, S. Neophytides and P. Lianos, *Sol. Energy Mater. Sol. Cells*, 2010, **94**, 592–597.
30 M. Antoniadou, P. Bouras, N. Strataki and P. Lianos, *Int. J. Hydrogen Energy*, 2008, **33**, 5045–5051.
31 P. Lianos, *J. Hazard. Mater.*, 2011, **185**, 575–590.

32 V. Cristino, S. Caramori, R. Argazzi, L. Meda, G. L. Marra and C. A. Bignozzi, *Langmuir*, 2011, **27**, 7276–7284.
33 X. Lu, D. Zheng, P. Zhang, C. Liang, P. Liu and Y. Tong, *Chem. Commun.*, 2010, **46**, 7721–7723.
34 J. Gan, X. Lu, T. Zhai, Y. Zhao, S. Xie, Y. Mao, Y. Zhang, Y. Yang and Y. Tong, *J. Mater. Chem.*, 2011, **21**, 14685–14692.
35 B. Zhou, M. Schulz, H. Y. Lin, S. I. Shah, J. Qu and C. P. Huang, *Appl. Catal., B*, 2009, **92**, 41–49.
36 P. Panagiotopoulou, M. Antoniadou, D. I. Kondarides and P. Lianos, *Appl. Catal., B*, 2010, **100**, 124–132.
37 B. Kraeutler and A. J. Bard, *J. Am. Chem. Soc.*, 1978, **100**, 2239–2240.
38 O. A. Semenikhin, V. E. Kazarinov, L. Jiang, K. Hashimoto and A. Fujishima, *Langmuir*, 1999, **15**, 3731–3737.
39 P. J. Barczuk, A. Lewera, K. Miecznikowski, P. Kulesza and J. Augustynski, *Electrochem. Solid-State Lett.*, 2009, **12**, B165–B166.
40 R. R. Davda, J. W. Shabaker, G. W. Huber, R. D. Cortright and J. A. Dumesic, *Appl. Catal., B*, 2005, **56**, 171–186.
41 M. Salari, K. Konstantinov and H. K. Liu, *J. Mater. Chem.*, 2011, **21**, 5128–5133.
42 X. Fu, J. Long, X. Wang, D. Y. C. Leung, Z. Ding, L. Wu, Z. Zhang, Z. Li and X. Fu, *Int. J. Hydrogen Energy*, 2008, **33**, 6484–6491.
43 X. H. Hao, L. J. Guo, X. Mao, X. M. Zhang and X. J. Chen, *Int. J. Hydrogen Energy*, 2003, **28**, 55–64.
44 M. R. St. John, A. J. Furgala and A. F. Sammells, *J. Phys. Chem.*, 1983, **87**, 801–805.
45 M.-H. Du, J. Feng and S. B. Zhang, *Phys. Rev. Lett.*, 2007, **98**, 066102.
46 D. Wen, S. Guo, Y. Wang and S. Dong, *Langmuir*, 2010, **26**, 11401–11406.
47 W. Y. Gan, D. Friedmann, R. Amal, S. Zhang, K. Chiang and H. Zhao, *Chem. Eng. J.*, 2010, **158**, 482–488.
48 M. Matsumura, M. Hiramoto, T. Iehara and H. Tsubomura, *J. Phys. Chem.*, 1984, **88**, 248–250.
49 H. Chum, M. Ratcliff, F. Posey, J. Turner and A. Nozik, *J. Phys. Chem.*, 1983, **87**, 3089–3093.
50 Y. X. Gan, B. J. Gan and L. Su, *J. Mater. Sci. Eng. B*, 2011, **176**, 1197–1206.